Reducing delamination of an electron-transporting polymer from a metal oxide for electrochemical applications

Aiswarya Abhisek Mohapatra,[a] Waleed Kuar Yual,[b] Yadong Zhang,[a] Anton Aleksandrovich Samoylov,[c] Jonathan Thurston,[d] Casey M. Davis,[d] Declan P. McCarthy,[d] Adam D. Printz,[c] Michael F. Toney,[a,e,f] Erin L. Ratcliff,[c] Neal R. Armstrong,[b] Ann L. Greenaway,[g] Stephen Barlow,[a,g*] and Seth R. Marder[a,d,f,g*]

[a]*Renewable and Sustainable Energy Institute, University of Colorado-Boulder, Boulder, CO, 80309, USA*
[b]*Department of Chemistry & Biochemistry, University of Arizona, Tucson, AZ, 85721, USA*
[c]*Department of Chemical and Environmental Engineering, University of Arizona, Tucson, AZ, 85721, USA*
[d]*Department of Chemistry, University of Colorado-Boulder, Boulder, CO, 80309, USA*
[e]*Department of Chemical and Biological Engineering, University of Colorado, Boulder, CO 80309, USA*
[f]*Materials Science and Engineering, University of Colorado, Boulder, CO 80309, USA*
[g]*National Renewable Energy Laboratory, Golden, CO, 80401, USA*

**Corresponding authors: seth.marder@colorado.edu, stephen.barlow@colorado.edu*

Table of contents:

Materials and Synthesis:

Materials

N2200 was purchased from 1-Materials (M_w = 140 kDa). ITO/glass with sheet resistance of 10 ohm/square was purchased from Colorado Concepts Coatings, USA. 2,2,2-Trifluoroethanol (TFE) and 1,2-dichlorobenzene (oDCB) (reagent grade) were purchased from Aldrich and was used without any further purification. Benzylphosphonic acid (BPA) (purity >97%) was purchased from Aldrich. All other solvents and chemicals were received from commercial sources and used without further purification.

Synthesis of Azido PA

Diethyl (2-hydroxyethyl)phosphonate (**2,** Scheme S1**)** was synthesized according to literature procedures.[1]

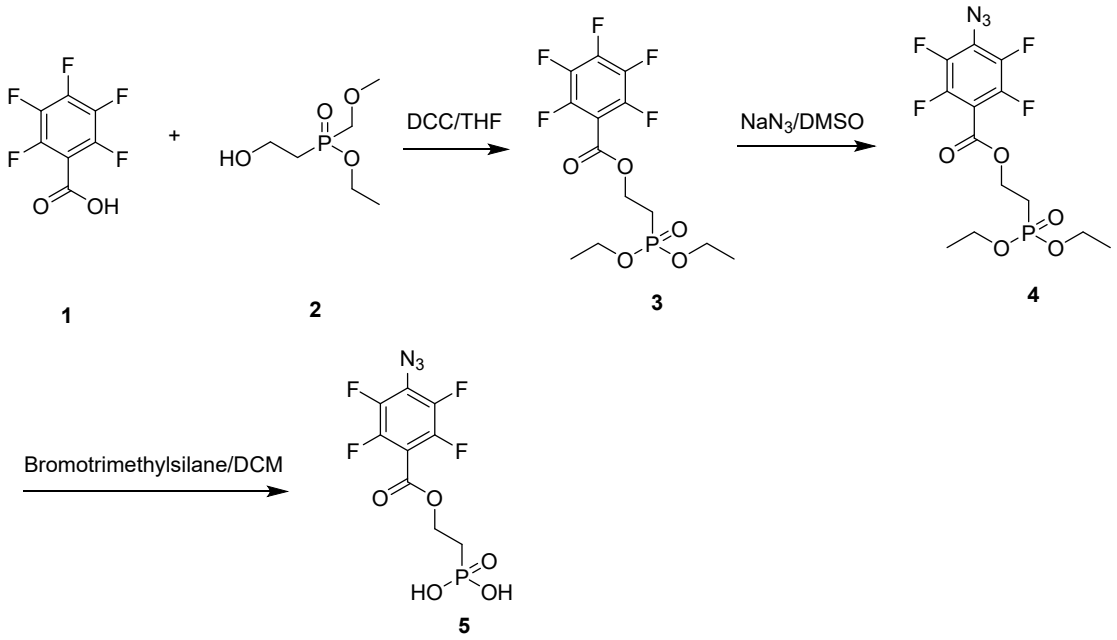

*Scheme S1. Synthesis of Azido PA (**5**).*

Diethyl (2-(2,3,4,5,6-pentafluorobenzoate)ethyl)phosphonate (**3**): To a solution of pentafluorobenzoic acid (2.0 g, 9.4 mmol), 2-hydroxy-ethyl-1-phosphonate (1.7 g, 9.3 mmol) and DMAP (20 mg, 0.16 mmol) in dry DCM (20.0 mL) was slowly added DCC (2.0 g, 9.7 mmol) at room temperature under nitrogen. The reaction mixture was stirred at room temperature for 1 h. White insoluble solid was removed by filtration. DCM was removed under reduced pressure and the crude product was purified by silica gel column chromatography using DCM/methanol (9:1) as eluent. After removal of solvents, a colorless liquid product was obtained, and dried in vacuum to afford the product (2.8 g, 80%).

^{1}H NMR (400 MHz, $CDCl_3$,): δ4.63 (m, 2H), 4.15 (m, 4H), 2.30 (m, 2H), 1.36 (t, J = 8 Hz, 6H) ppm. ^{19}F NMR (376 Hz, $CDCl_3$): δ-137.85 (m, 2F), -147.98 (m, 1F), -160.15 (m, 2F) ppm. ^{31}P NMR (162 MHz, $CDCl_3$): δ25.50 (s) ppm. ^{13}C{^{1}H} NMR (100 MHz, $CDCl_3$): δ158.68 (m), 145.44 (dm, $J_{C\text{-}F}$ = 259.0 Hz), 143.22 (dm, $J_{C\text{-}F}$ = 259.0 Hz), 137.75 (dm, $J_{C\text{-}F}$ = 259.0 Hz), 107.83 (m), 61.98 (d, $J_{C\text{-}P}$ = 6.0 Hz), 60.97, 25.95 (d, $J_{C\text{-}P}$ = 140.0 Hz), 16.32 ($J_{C\text{-}P}$ = 6.0 Hz) ppm. HRMS-ESI, Calculated for $C_{13}H_{15}F_5O_5P$ (MH^+): m/z = 377.0572; Found: m/z = 377.0577. Anal. Calculated for $C_{13}H_{14}F_5O_5P$: C, 41.50; H, 3.80; N, 0.00. Found: C, 41.23; H, 3.80; N, 0.00.

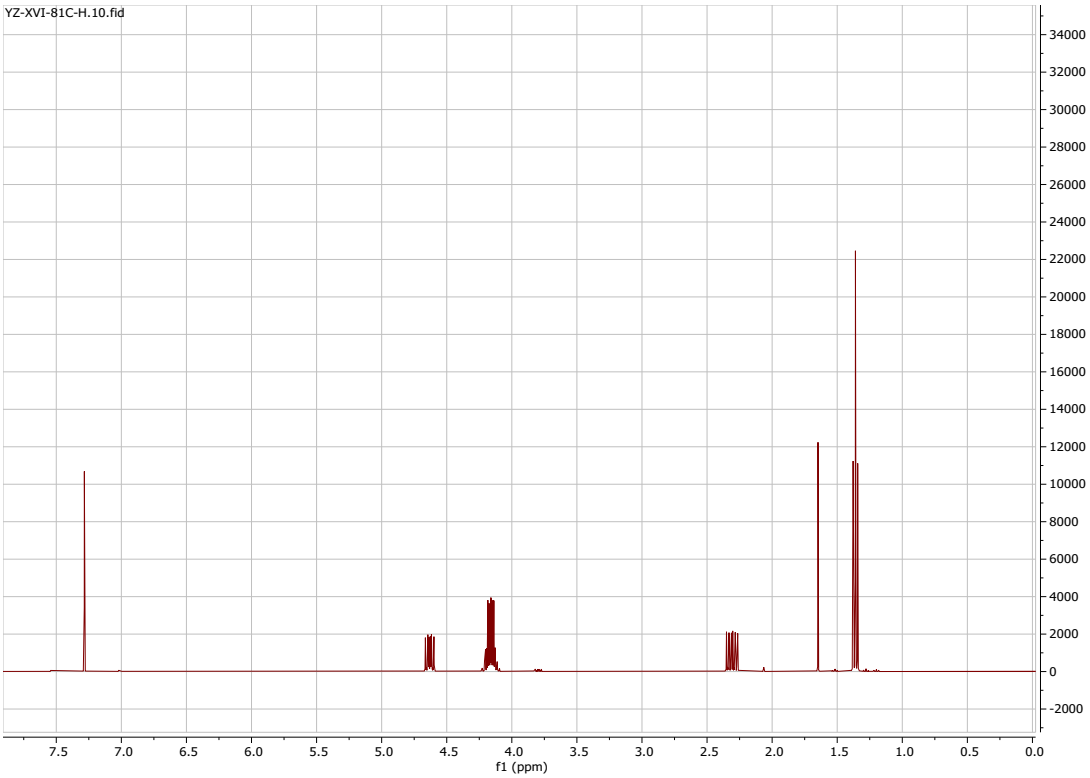

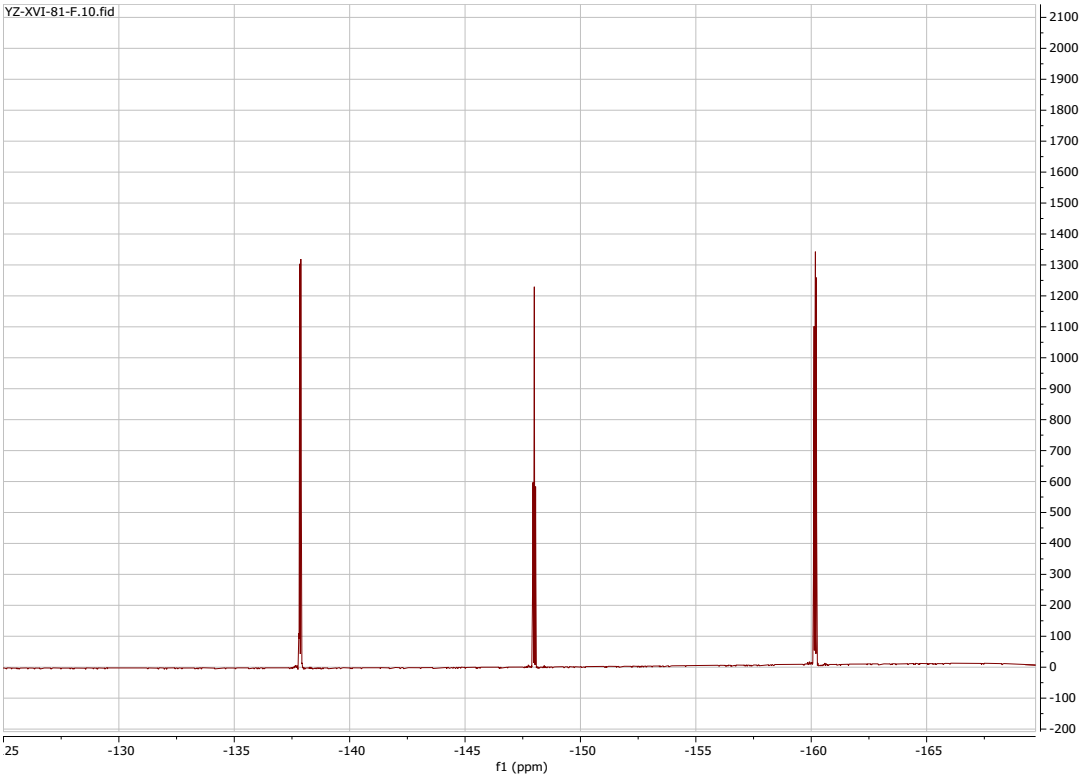

*Fig. S1. ^{1}H (top) and ^{19}F (bottom) NMR spectra of **3** in $CDCl_3$ and DMSO-d_6 respectively.*

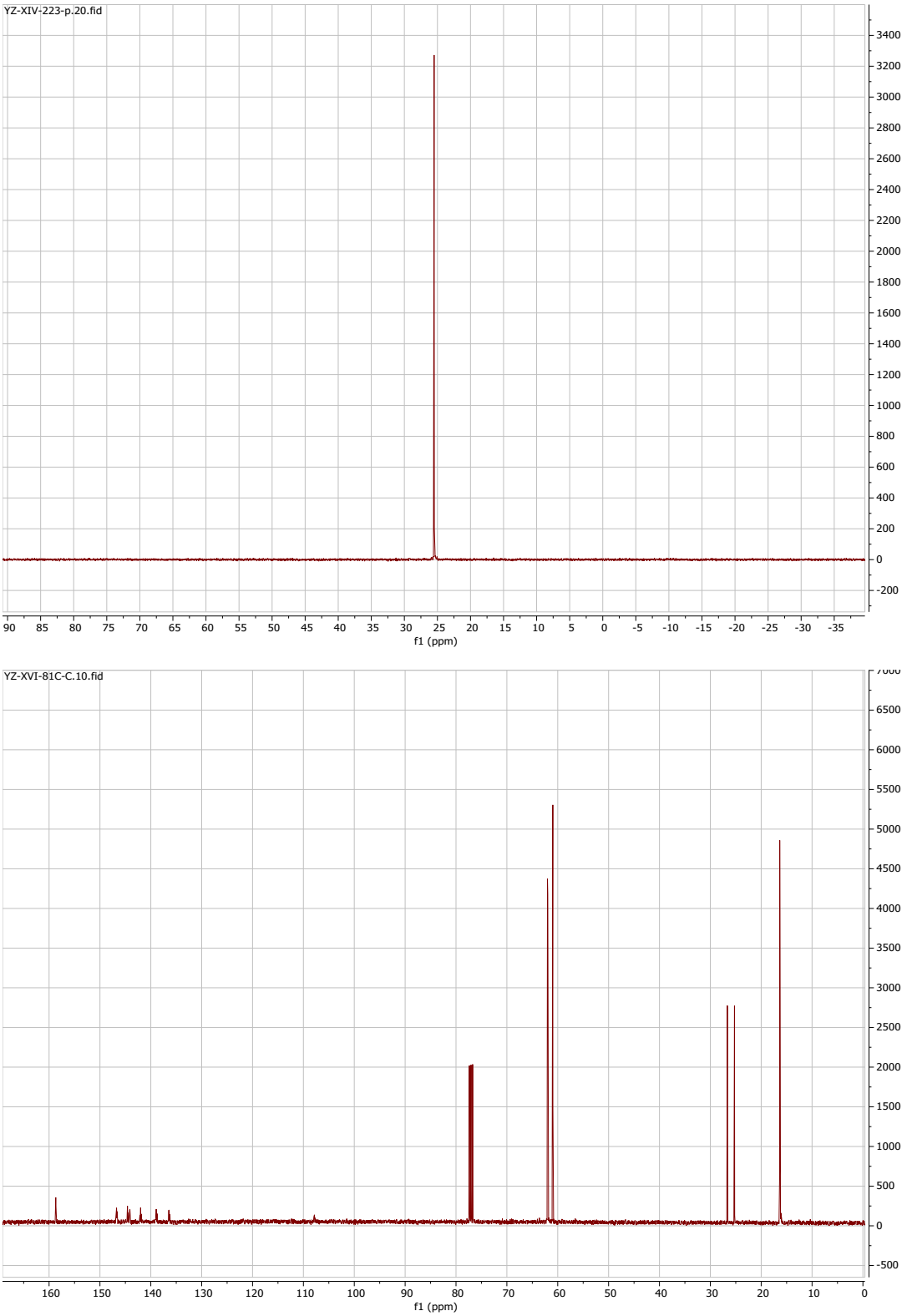

Fig. S2. ^{31}P (top) and $^{13}C\{^{1}H\}$ (bottom) NMR spectra of **3** in DMSO-d_6 and $CDCl_3$ respectively.

Diethyl (2-(4-azido-2,3,5,6-tetrafluorobenzoate)ethyl)phosphonate (4):

To a solution of diethyl (2-(2,3,4,5,6-pentafluorobenzoate)ethyl)phosphonate (**3**) (2.0 g, 5.3 mmol) in DMSO (10.0 mL) was slowly added sodium azide (0.35 g, 5.4 mmol) at room temperature. The reaction mixture was stirred at room temperature for 4 h. Water (100 mL) was added into the reaction mixture. The product was extracted with DCM and the organic extracts were washed with water. After removal of solvent, the crude product was purified with column chromatography on silica gel using DCM/methanol (9 :1) as the eluent. After removal of solvent, the product pale-yellow liquid was dried under vacuum to afford pure product (2.1 g, 100%).

^{1}H NMR (400 MHz, $CDCl_3$): δ4.62 (m, 2H), 4.15 (m, 4H), 2.30 (m, 2H), 1.36 (t, J = 4.0 Hz, 6H) ppm. ^{19}F NMR (376 Hz, $CDCl_3$): -138.38 (m, 2F), -150.80 (m, 2F) ppm. ^{31}P NMR (162 MHz, $CDCl_3$): δ25.62 (s) ppm. ^{13}C{^{1}H} NMR (100 MHz, $CDCl_3$): δ158.96 (m), 145.30 (dm, $J_{C\text{-}F}$ = 259.0 Hz), 140.29 (dm, $J_{C\text{-}F}$ = 259.0 Hz), 123.59 (m), 107.29 (t, $J_{C\text{-}F}$ = 15 Hz), 61.98 (d, $J_{C\text{-}P}$ = 6.0 Hz), 60.75, 25.95 (d, $J_{C\text{-}P}$ = 140.0 Hz), 16.33 ($J_{C\text{-}P}$ = 6.0 Hz) ppm. HRMS-ESI, Calculated for $C_{13}H_{15}F_4N_3O_5P$ $(MH)^+$: *m/z* = 400.0680; Found: *m/z* = 400.0889. Anal. Calculated for $C_{13}H_{14}F_4N_3O_5P$: C, 39.11; H, 3.53; N, 10.53. Found: C, 38.94; H, 3.57; N, 10.67.

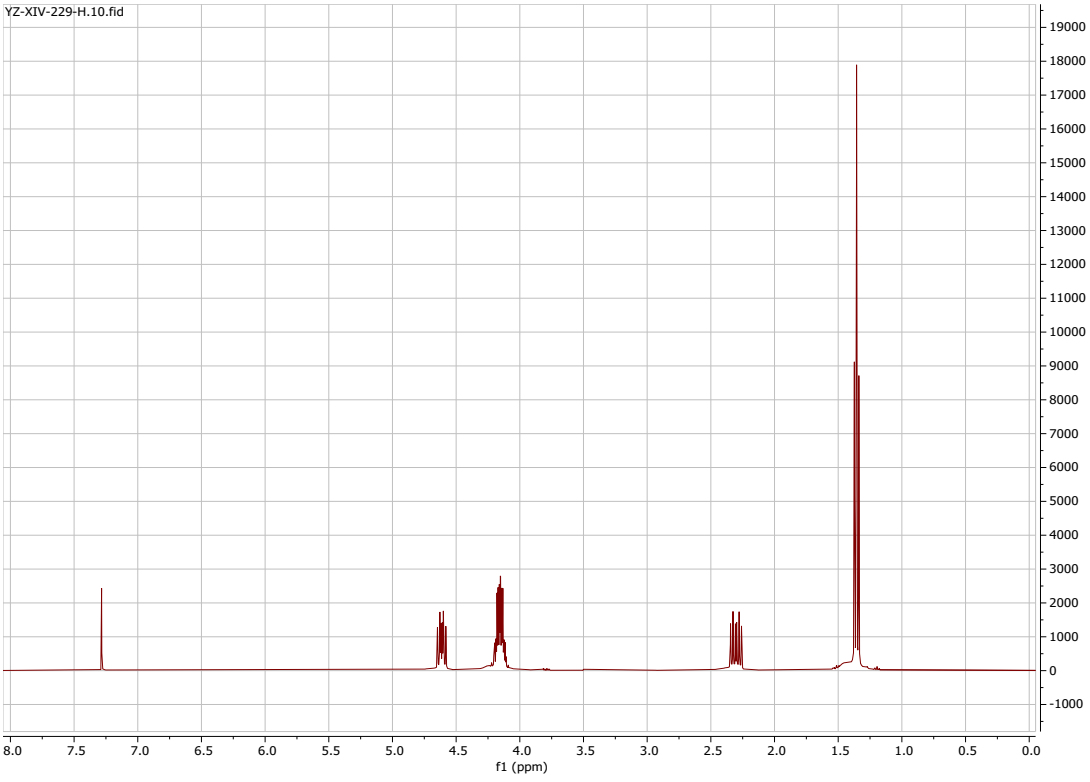

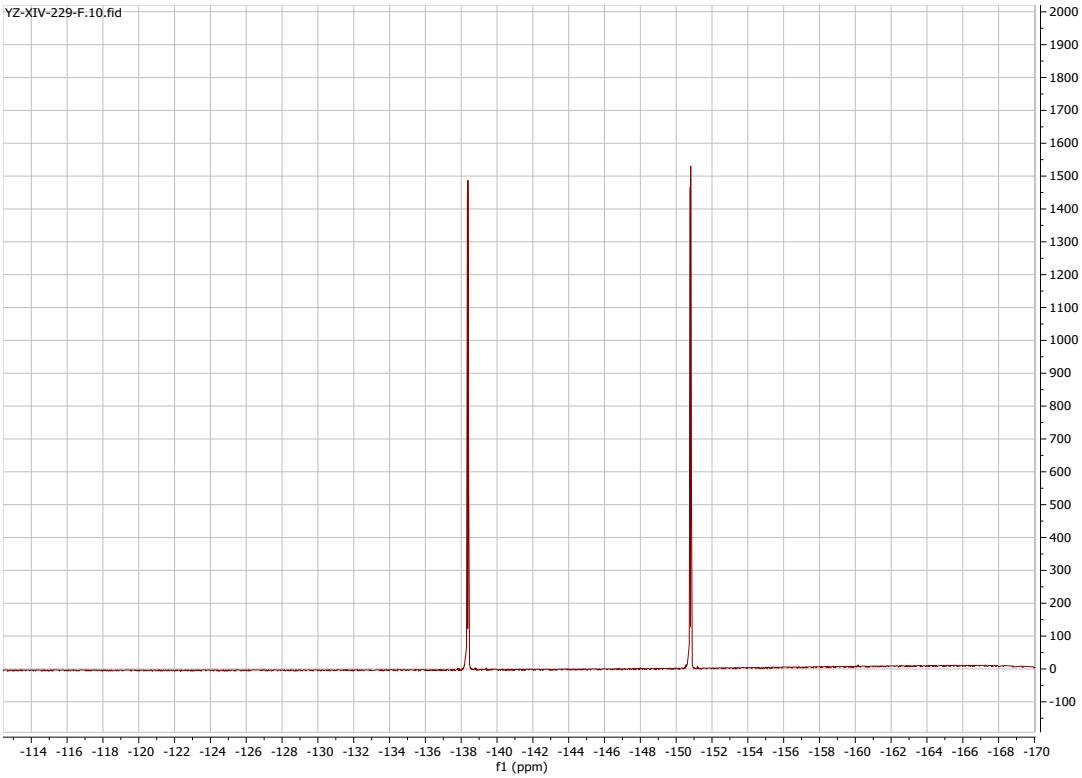

*Fig. 3. ^{1}H (top) and ^{19}F (bottom) NMR spectra of **4** in $CDCl_3$.*

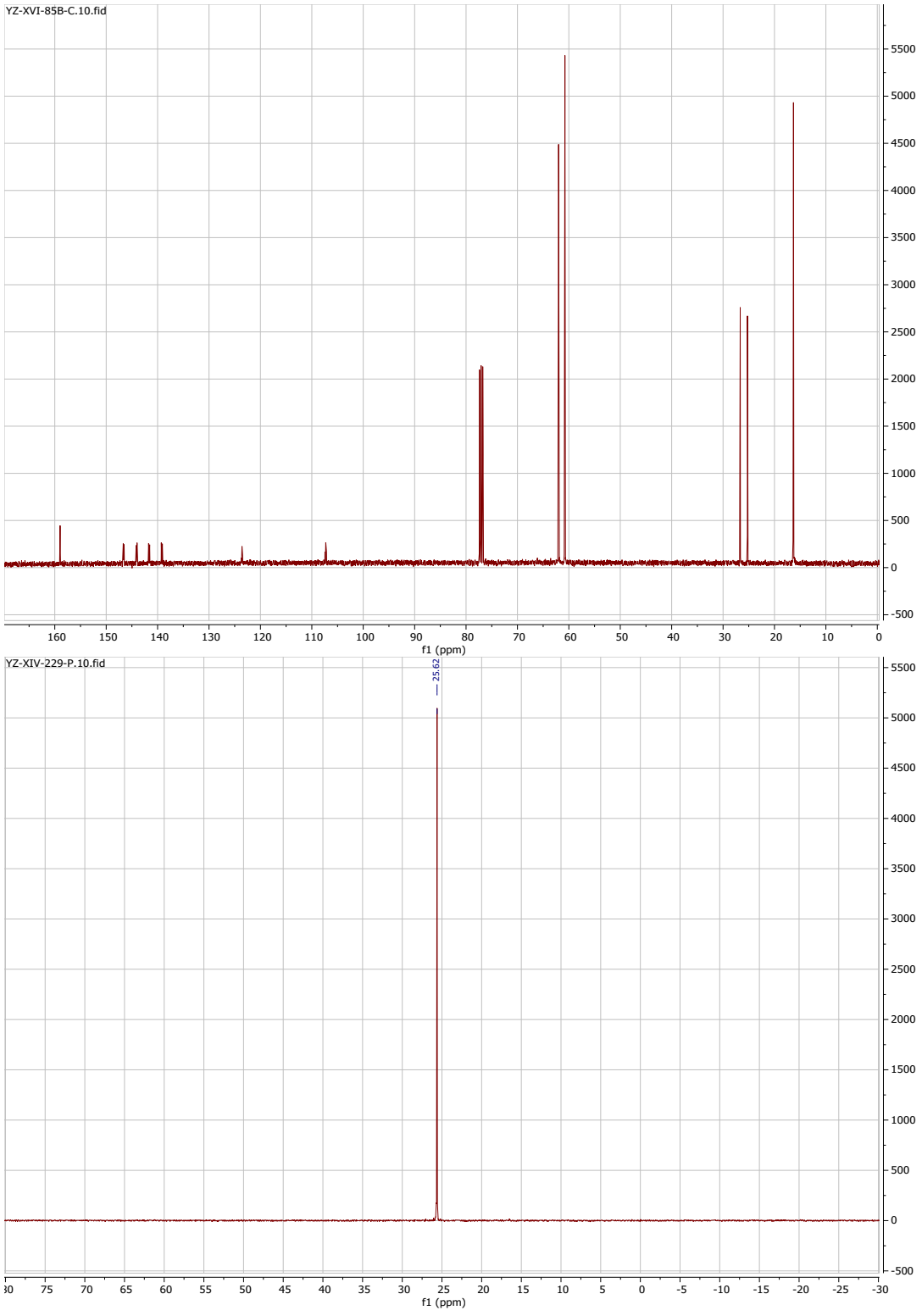

Fig. S4. ^{31}P *(top) and* $^{13}C\{^{1}H\}$ *(bottom) NMR spectra of* ***4*** *in* $CDCl_3$.

(2-(4-Azido-2,3,5,6-tetrafluorobenzoate)ethyl)phosphonic acid (5):

To a solution of diethyl (2-(4-azido-2,3,5,6-tetrafluorobenzoate)ethyl)phosphonate (**4**) (1.8 g, 4.5 mmol) in DCM (20.0 mL) was added bromotrimethylsilane (6.0 g, 39.2 mmol) under nitrogen at room temperature. The reaction mixture was stirred at room temperature for 22 h. Methanol (20.0 mL) was added, the solution was stirred at room temperature for 60 min. DCM was removed under reduced pressure and water (20.0 mL) was added into the methanol solution. Methanol was removed under reduced pressure and the resulting white solid was collected with filtration, washed with water, and dried under vacuum (1.3 g, 87%) yield.

^{1}H NMR (400 MHz, DMSO-d_6): δ8.70 (s, br, 2H), 4.40 (m, 2H), 1.99 (m, 2H) ppm. ^{19}F NMR (376 Hz, DMSO-d_6): δ-140.15 (m, 2F), -151.38 (m, 2F) ppm. ^{31}P NMR (162 MHz, DMSO-d_6): δ19.86 (s) ppm. ^{13}C{^{1}H} NMR (100 MHz, DMSO-d_6): δ159.13 (m), 145.12 (dm, $J_{C\text{-}F}$ = 259.0 Hz), 140.66 (dm, $J_{C\text{-}F}$ = 259.0 Hz), 124.25 (m), 106.86 (t, $J_{C\text{-}F}$ = 15 Hz), 62.20 (d, $J_{C\text{-}P}$ = 1.0 Hz), 28.12 (d, $J_{C\text{-}P}$ = 133.0 Hz) ppm. HRMS-ESI, Calculated for $C_9H_5F_4N_3O_5P$ $(M\text{-}H)^-$, $(2M\text{-}H)^-$: *m/z* = 341.9908, 684.9890; Found: *m/z* = 341.9903, 684.9883. Anal. Calculated for $C_9H_6F_4N_3O_5P$: C, 31.50; H, 1.76; N, 12.25. Found: C, 31.60; H, 1.60; N, 12.21.

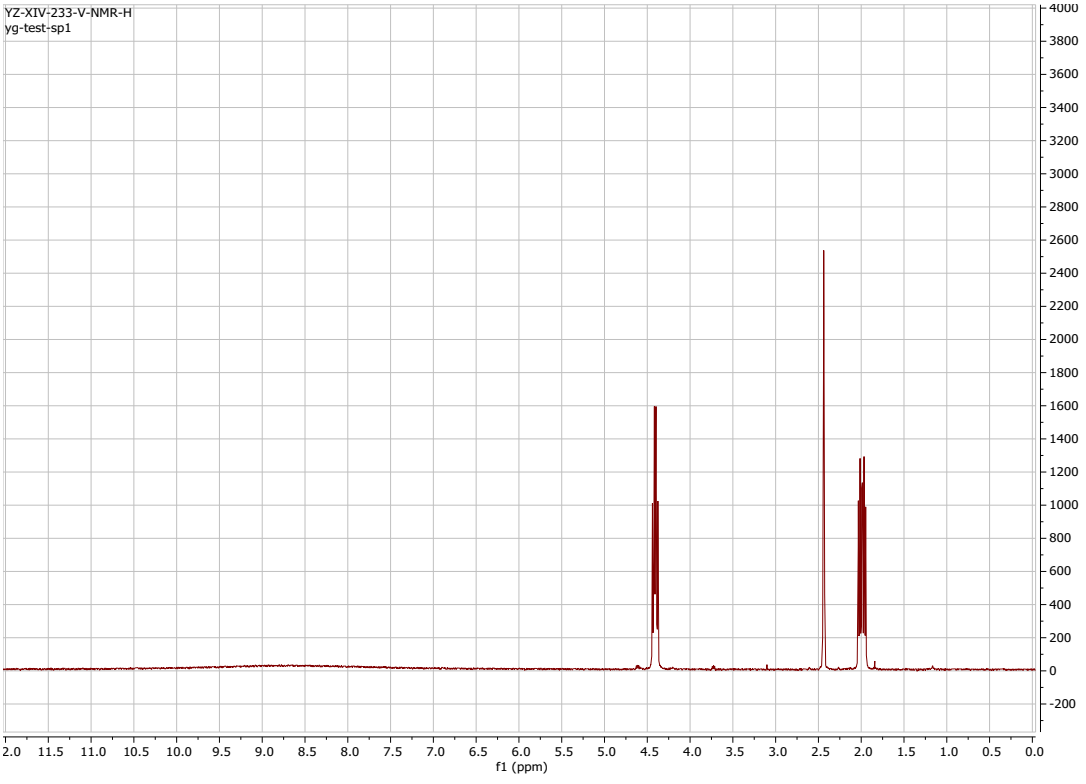

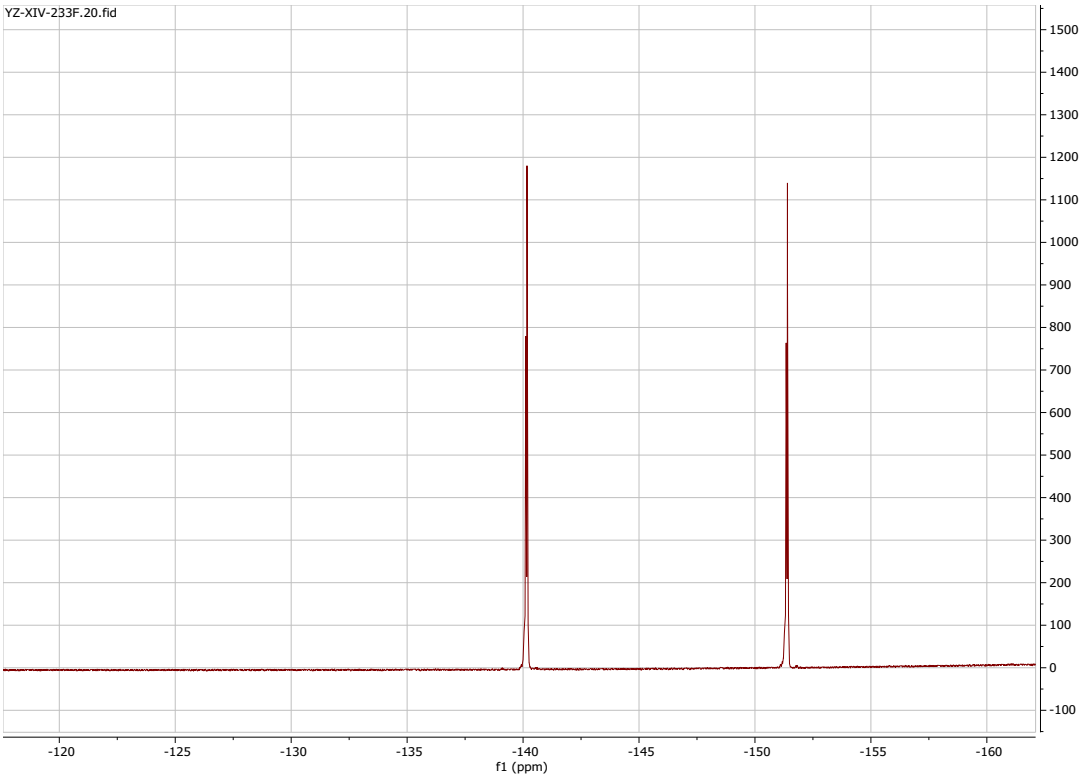

*Fig. S5. ^{1}H (top) and ^{19}F (bottom) NMR spectra of **5** in DMSO-d_6.*

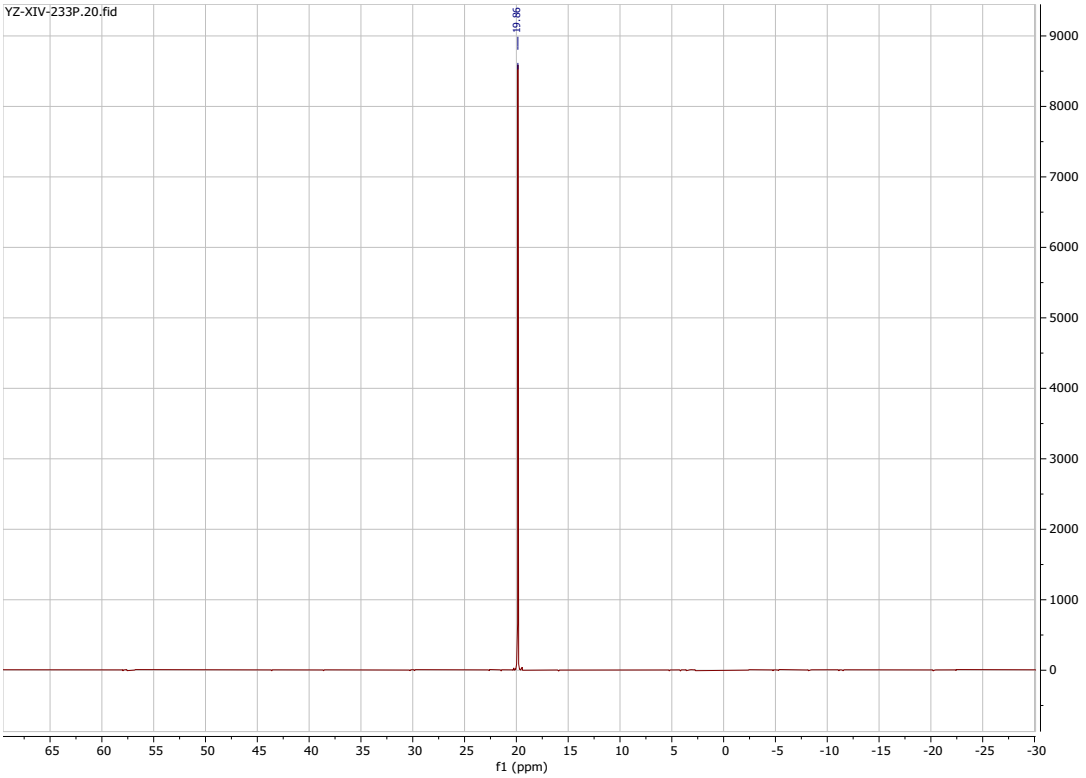

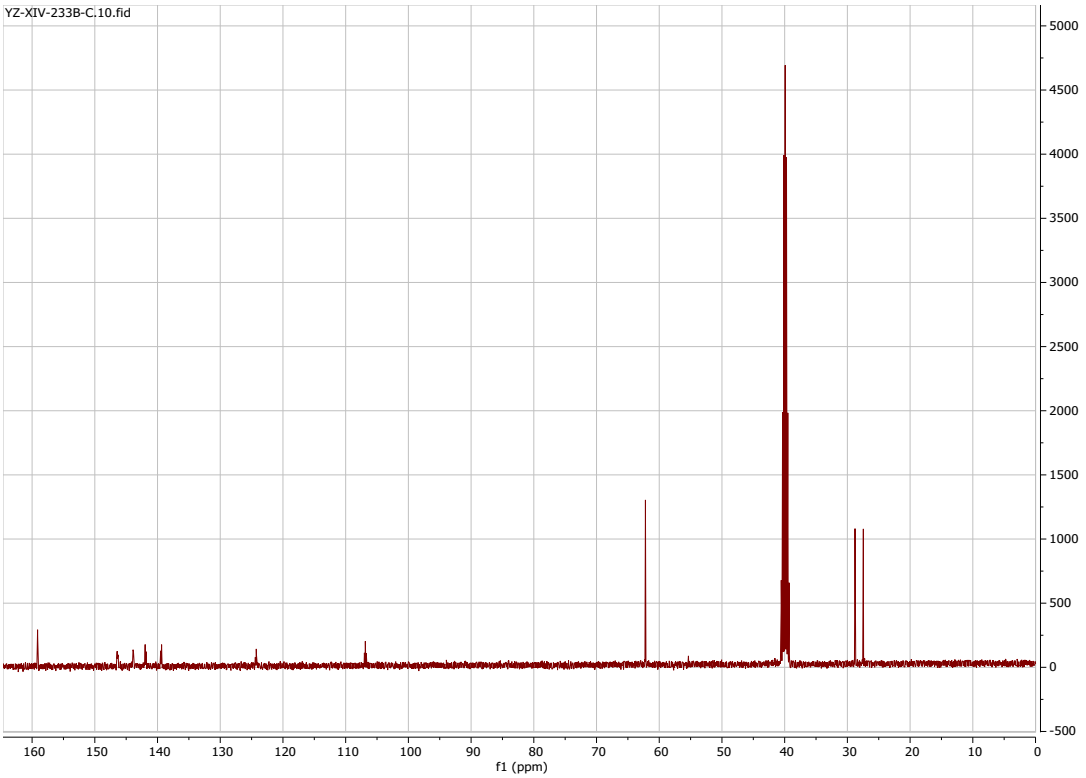

*Fig. S6. ^{31}P (top) and $^{13}C\{^{1}H\}$ (bottom) NMR spectra of **5** in DMSO-d_6.*

Preparation of N2200 films on phosphonic acid modified ITO

The ITO substrates were cleaned by subsequent sonication in soap water, DI water, acetone, and IPA for 10 min each. Before depositing the PAs, ITO substrates were blow dried using an air gun and UV-ozone treatment was performed for 10 min. The phosphonic acids (PAs) were dissolved in TFE (0.3 mg/mL) at 50 ˚C for 6 h and spun coated on 5 mm × 5 mm ITO/glass at 3000 rpm for 60 s after soaking in the for 25 s, followed by annealing at 80 ˚C for 5 min. Subsequently, the substrates were washed twice, dynamically, using TFE at 6000 rpm for 60 s. N2200 solution was prepared by dissolving the required amount of polymer in oDCB and stirring the solution at 80 ˚C for at least 8 h. in ambient conditions. To get 10 nm thick films, 7 mg/mL N2200 solution was spin-coated at 3500 rpm for 60 s. To get 100 nm thick films, 15 mg/mL N2200 solution was spin-coated at 1400 rpm for 60 s. All the films were annealed at 110 ˚C for 10 min.

Photo-tethering of Azido PA

Photo-tethering was performed for the Azido PA tethered films by shining UV light from the ITO side for 5 min. To check the solvent resistance, the films were dipped in oDCB at 160 ˚C for 5 min followed by ultrasonication in oDCB in a water bath for 2 min. Ultimately, they were blow-dried using an air-gun before collecting the UV-vis absorption spectrum.

Characterization Methods:

NMR spectroscopy

^{1}H, ^{13}C, ^{19}F, and ^{31}P-NMR spectra were recorded with Bruker Avance 400 MHz spectrometer.

ESI-mass spectroscopy

ESI mass spectra were provided by the University of Colorado Boulder mass spectra facility laboratory. Elemental analyses were obtained from Atlantic Microlab.

X-ray and UV photoelectronic spectroscopy

The PA coated ITO samples were kept in vacuum prior to insertion into a Kratos XPS chamber. Al Kα (1486.6 eV) was used as a high energy excitation source for XPS. For UPS, He Kα source was used as the excitation source.

Contact angle measurement

Contact angle (CA) measurements were performed to determine the surface energies of the PA derivatives as well as N2200 on ITO. DI water was used as the polar liquid and diiodomethane as dispersive one. Average CAs from five consecutive measurements were recorded for all the samples. The surface energies were determined using both geometric and harmonic mean methods (see Table 1).

Cyclic voltammetry and spectroelectrochemistry in aqueous medium

For cyclic voltammetry (CV), N2200 coated ITO was used as the working electrode, Ag/AgCl in 0.1 M KCl as the reference and Pt wire was used as the counter electrode. 0.1 M KCl was used as electrolyte, 1 mM HCl was added to achieve pH 3 and 1 mM NH_4OH was added to achieve pH 11. The electrolyte solution was degassed using a nitrogen line for 15 min before performing electrochemistry. CV was performed in standard three electrode configuration using a CH Instruments CH920D bipotentiostat. A scan rate of 25 mV/s was used for both cyclic voltammograms and spectroelectrochemistry experiments. All spectroelectrochemistry experiments were measured with an Agilent 8453 spectrophotometer in conjunction with the CH instruments CH920D bipotentiostat. A diagram of the electrochemical compression cell used for the measurements is shown in Fig. S7.

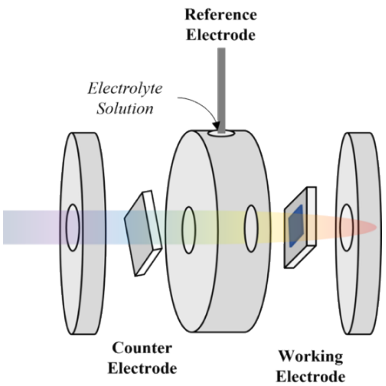

Fig. S7. Electrochemical compression cell used for aqueous spectroelectrochemistry.

Spectroelectrochemistry in non-aqueous medium

Non-aqueous spectroelectrochemistry was performed using a Redox.me cell equipped with optical waveguides. The N2200 thin films on ITO were mounted as working electrodes with 1 cm^2 exposed areas; a coiled Pt wire was used as a counter electrode and the reference pseudo electrode was an Ag wire. The supporting electrolyte was 100 mM tetrabutylammonium hexafluorophosphate ($TBAPF_6$) dissolved in acetonitrile. CVs were performed using a BioLogic potentiostat at 20 mV/s. The illumination source was an OceanOptics DH-2000 with a halogen bulb, and the evolution of the UV-Vis spectra was monitored using a OceanOptics flame spectrometer and OceanView software. Following spectroelectrochemical measurements, equal concentrations of ferrocene and ferrocenium were added to the supporting electrolyte and CVs were repeated in order to provide the reference potential. For data analysis, the absorbance spectrum of the thin film at the beginning of the second CV cycle was taken as the baseline.

UV-visible absorption spectroscopy

The UV-vis absorption spectra of all the films were recorded in transmission mode using a Cary 5000 UV-Vis-NIR Spectrophotometer.

Film thickness measurement using Dektak profilometer

The average thickness of the N2200 films were measured using Dektak surface profilometer with a tip diameter of 2 µm with an applied force of 2 mg.

Fracture energy measurement

The fracture energy of the N2200 on surface modified ITO specimens were measured using the double cantilever beam (DCB) method. Glass substrates were cut using a diamond-tipped scribe from 75 mm × 25 mm × 1 mm glass substrates (Fisherbrand, purchased from Fisher Scientific) into 37.5 mm × 25 mm × 1 mm coupons. The resulting coupons were cleaned by sonicating in subsequent baths of 1% Alconox and water, deionized (DI) water, acetone, and isopropyl alcohol (IPA) for 10 min each. Substrates were dried using compressed nitrogen to prepare them for sputter coating of a ITO surrogate film. A Kurt J. Lesker Axxis sputter coater was used to deposit 150 nm of the ITO surrogate which was then annealed at 350 °C for 1 h in air. XPS (Figs S13-15) indicates has a higher Sn:In ratio than usual, which should not, however, affect our results since PAs bind strongly to wide variety of metal-oxides including SnO_2-like compositions such as FTO. The oxide-coated coupons were re-washed according to the steps listed above and plasma treated in oxygen for 10 min at 120 W to increase the wettability of the substrates prior to polymer deposition.

The azido PAs were activated to tether to the N2200 by UV light; to determine the influence of the UV light on the N2200 films, we subjected all specimens to three conditions: (1) no UV exposure; (2) UV exposure through the N2200 side of the specimen; and (3) UV exposure through the IT-glass side of the specimen. The UV exposed specimens were placed below a short wave (254 nm) lamp for 5 minutes at a distance of 1 cm from the sample surface. A 200 nm thick layer of Al was deposited on top of the N2200 using e-beam deposition to form an encapsulation layer to prevent epoxy ingress into the film in the following step. Finally, a clean glass slide of the same size (37.5 mm × 25 mm) was adhered to the top of the Al layer using Loctite E-20NS HYSOL epoxy. These specimens were left in a nitrogen environment for 12 h at room temperature to allow the epoxy to fully cure before performing the DCB measurements.

Double cantilever beam testing (DCB) was performed in ambient conditions using a thin-film cohesion testing system (Delaminator DTS, Menlo Park, CA) which measured load, *P*, versus displacement, *Δ*. The initial displacement speed was set to 1 μm s^{-1}, which was increased linearly to accommodate the increasing crack length. The critical fracture energy, Gc (J m^{-2}), was then calculated from equation 1:

$$G_c = \frac{12P_c^2a^2}{b^2E^{'}h^3}\left(1 + 0.64\frac{h}{a}\right)^2 \quad (1)$$

Where P_c is the critical load at which crack growth occurs, a is the crack length, $E^{'}$ is the plane-strain elastic modulus, and b and h are the width and half-thickness of the substrates, respectively. The crack length was estimated from elastic compliance ($d\Delta/dP$) using equation 2:

$$a = \left(\frac{d\Delta}{dP} \times \frac{bE^{'}h^3}{8}\right)^{1/3} - 0.64h \quad (2)$$

Survey scans (0–1000 eV) were performed on the DCB fractured testing samples with X-ray photoelectron spectroscopy (XPS, Kratos Axis Ultra 165 Hybrid Photoelectron Spectrometer) using monochromatic Al Kα x-ray radiation at 1486.6 eV to determine the composition of chemical species at the surface of the fractured samples after DCB testing in five spots on each of the delaminated sides. The side of the fractured sample adhered to the slide glued with epoxy is referred to as the ‘‘Epoxy side’’ and the other side is referred to as the “ITO side.”

XPS Data for PA-modified ITO:

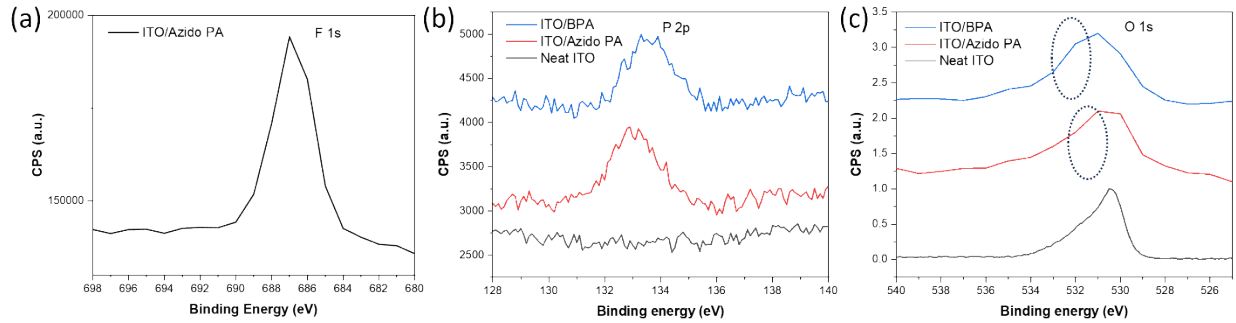

Fig. S8. XPS scans of (a) F 1s confirming the presence of Azido PA on ITO, (b) P 2p confirming the presence of BPA and Azido PA on ITO, (c) O 1s confirming the chemical linkage of the phosphonic acid group to the ITO surface through P-O-M bonds.

XPS was performed to probe the binding of PAs onto ITO as shown in Fig. S8, the presence of F 1s and P 2p peaks for Azido PA modified ITO and the presence of P 2p peak for BPA modified ITO is consistent with the presence of the PA on ITO surface (Fig. S8a, S8b). The shift of O 1s peak to higher binding energies (Fig. S8c) for the modified substrates is consistent with formation of P-O-M linkage to the ITO.[2,3]

Contact Angle and Work Function Data:

Table S1. Contact angle of water and diiodomethane (DIM) on ITO and modified ITO surfaces. The top row of surface energy is determined by harmonic mean method[4,5] and the bottom one by geometric mean method.[6,7]

	Contact angle (˚)		Surface energy (mN/m)		Work function (eV)
	Water	DIM	Dispersive	Polar	
ITO (UV-O_3 treated)	8.8	8.4	50	36	4.47
			50	30	
ITO/BPA	23.7	17.8	48	33	4.80
			48	27	
ITO/Azido PA	38.7	28.9	45	27	4.88
			45	22	
ITO/N2200	95.7	49.4	36	3	N/A
			35	0.5	

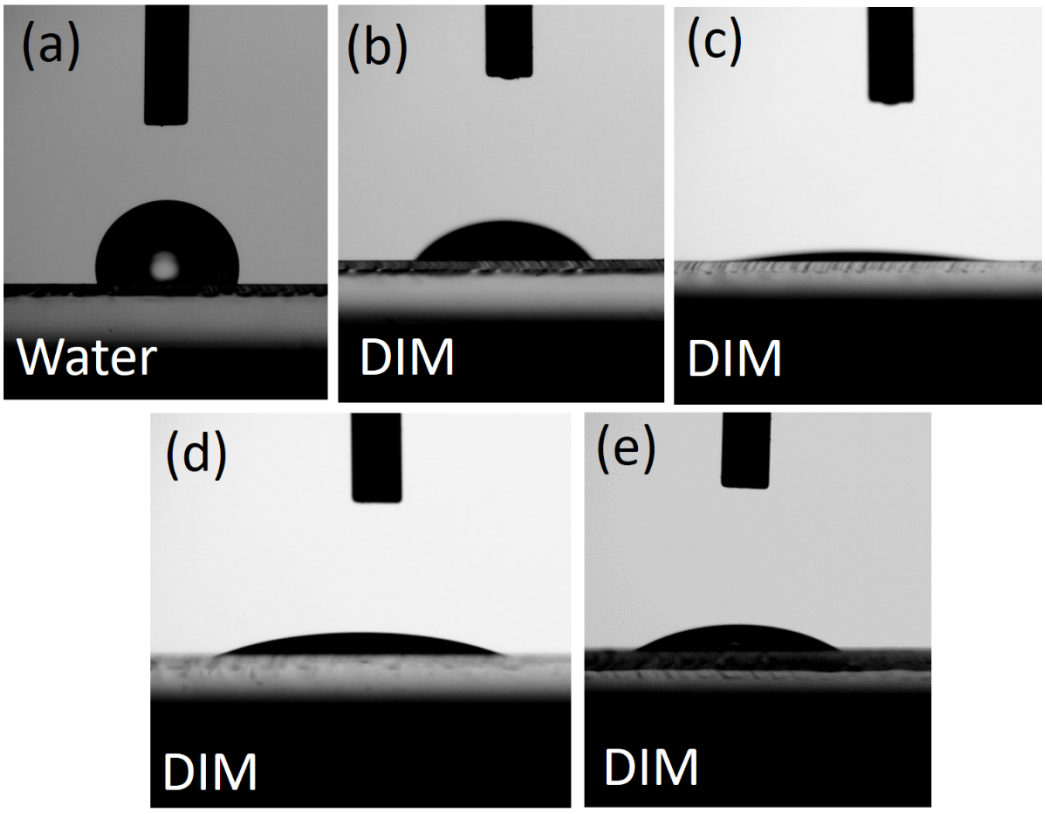

Fig. S9. Contact angle of water (a) and (b) diiodomethane (DIM) on ITO/N2200, contact angle of DIM on (c) UV-ozone treated ITO, (d) ITO/BPA, and (e) ITO/Azido PA.

UV-Vis. Data and Additional Aqueous Electrochemistry:

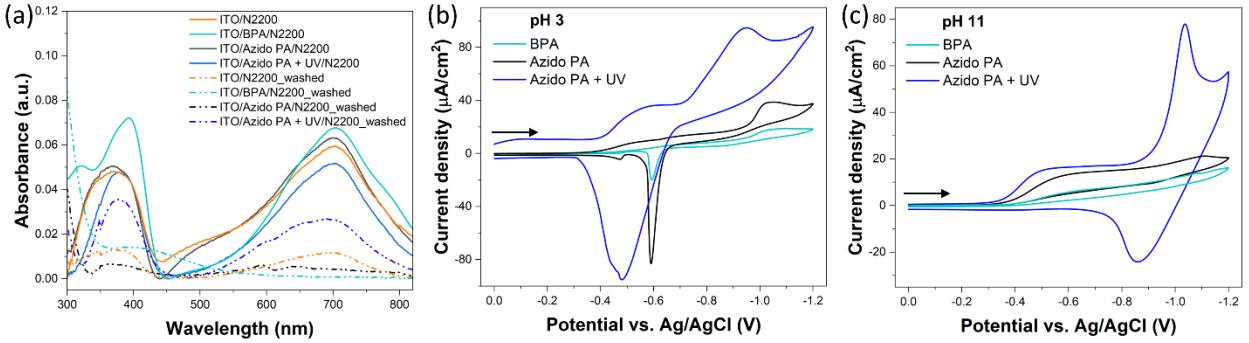

Fig. S10. (a) the UV-vis spectra of N2200 on unmodified ITO and ITO modified with BPA or with Azido PA, with or without UV exposure, before and after washing with oDCB at 160 °C. Cyclic voltammograms of 100 nm N2200 on BPA, Azido PA modified ITO, and Azido PA modified and photo-tethered in pH (b) 3 and (d) 11.

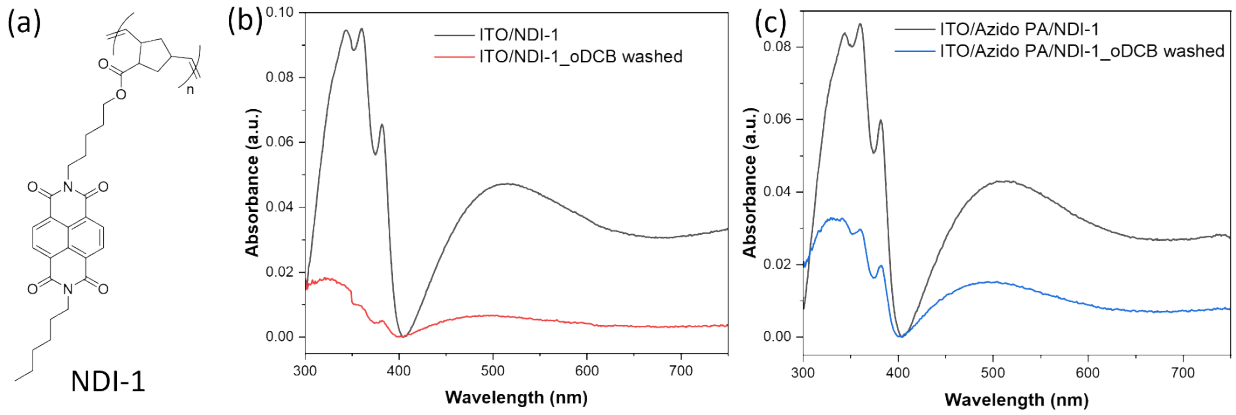

Fig. S11. (a) Chemical structure of naphthalene diimide based side-chain polymer (NDI-1); (b) UV-vis absorption spectra of the NDI-1 on unmodified ITO before and after washing in oDCB at 160 ˚C suggesting nearly complete removal of the film; (c) UV-vis absorption spectra of NDI-1 crosslinked on azido PA modified ITO before and after washing in oDCB at 160 ˚C showing ~45% retention.

Fracture-Energy Analysis:

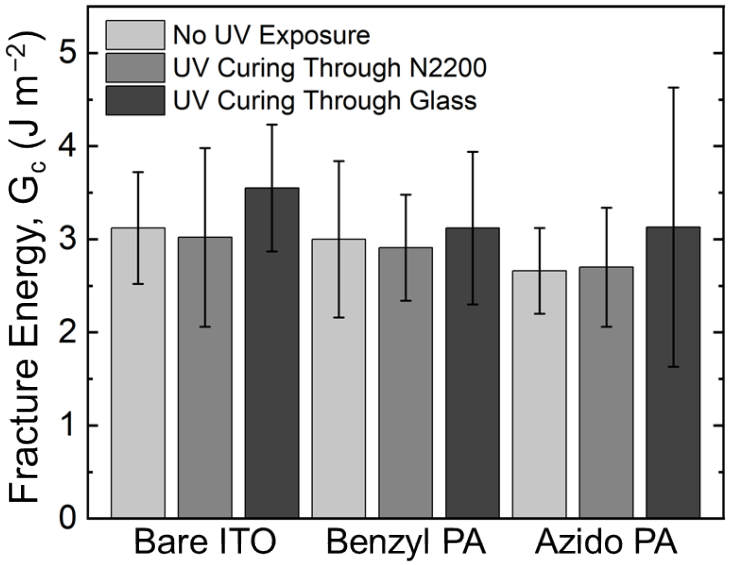

Fig. S12. Fracture energies for all the surface modifications and UV treatments. The similarity in values indicates that the delamination is not driven by poor mechanical adhesion.

Table S2. Fracture energies of various N2200 films with combinations of UV treatment and phosphonic acid surface modification.

N2200 Deposited Onto:	UV Curing	Average G_c (J m^{-2})
Pristine ITO	Through Glass	3.55 ± 0.68
	Through N2200	3.02 ± 0.96
	None	3.12 ± 0.60
ITO w/ Benzyl PA	Through Glass	3.12 ± 0.82
	Through N2200	2.91 ± 0.57
	None	3.00 ± 0.84
ITO w/ Azido PA	Through Glass	3.13 ± 1.50
	Through N2200	2.70 ± 0.64
	None	2.66 ± 0.46

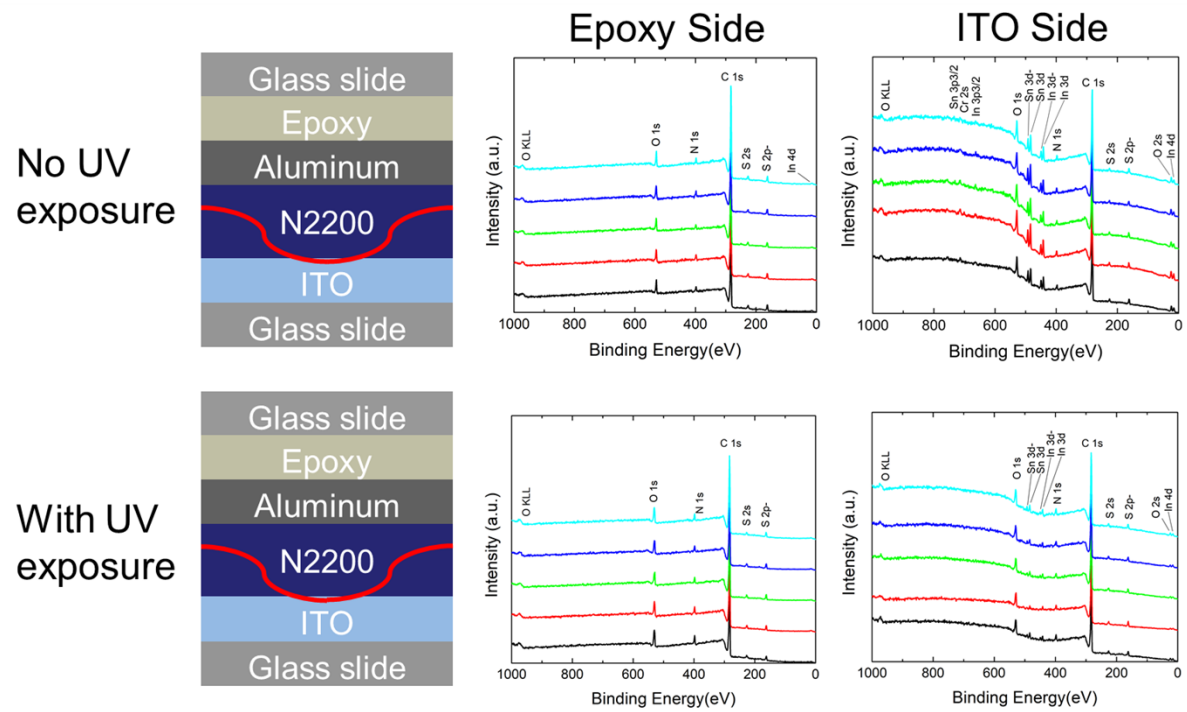

Fig. S13. Fracture path through specimens of N2200 on pristine ITO surrogate on glass as fabricated (top) and after exposure to UV (bottom). XPS measurements were taken on both the top ("epoxy") side and bottom ("ITO") side of the fractured specimen to determine the fracture path.

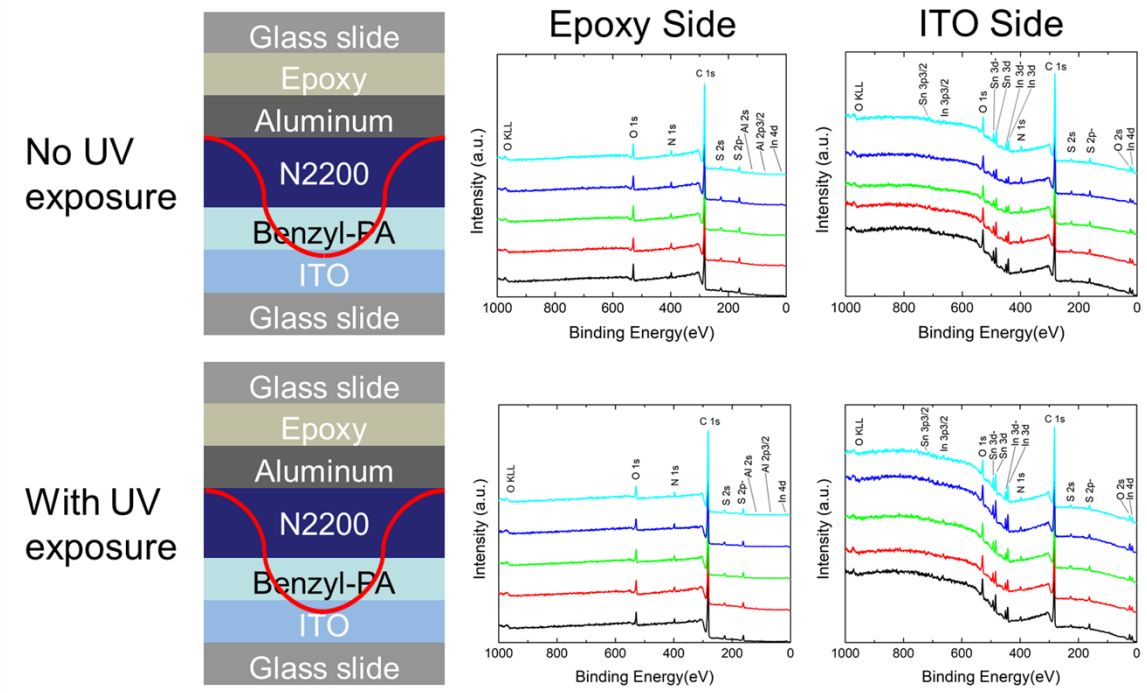

Fig. S14. Fracture path through specimens of N2200 on benzyl PA-modified ITO-surrogate on glass as fabricated (top) and after exposure to UV (bottom). XPS measurements were taken on both the top ("epoxy") and bottom ("ITO") side of the fractured specimen to determine the fracture path.

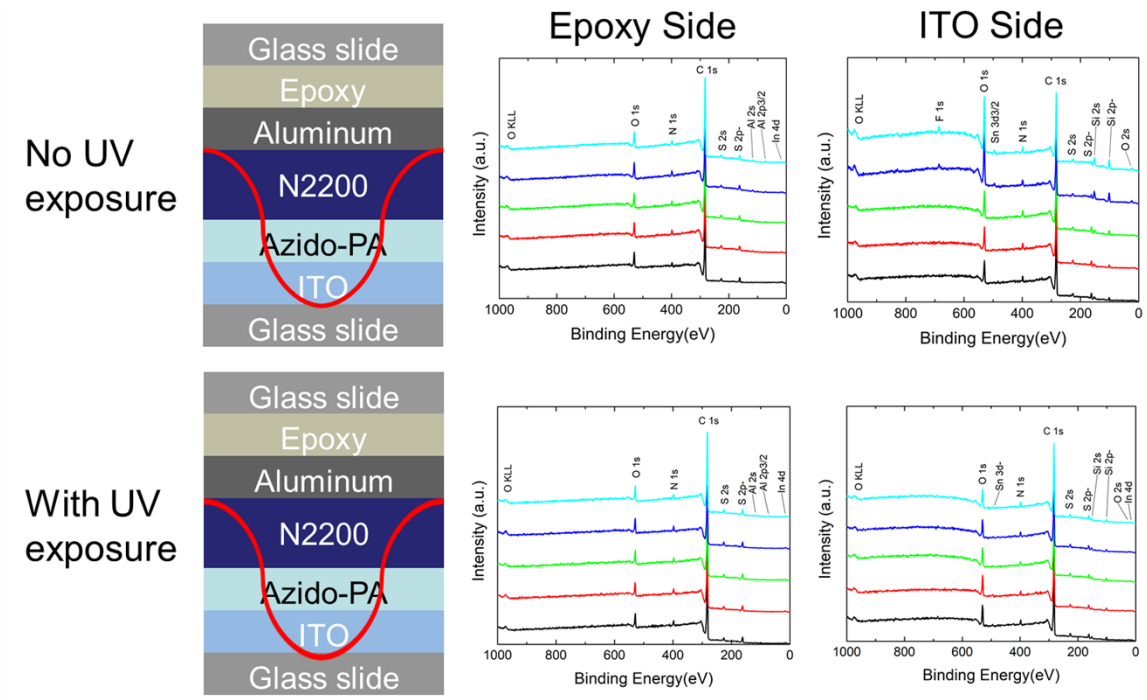

Fig. S15. Fracture path through specimens of N2200 on azido PA-modified surrogate ITO on glass as fabricated (top) and after exposure to UV (bottom). XPS measurements were taken on both the top ("epoxy") and bottom ("ITO") side of the fractured specimen to determine the fracture path.

Aqueous (Spectro)Electrochemical Data:

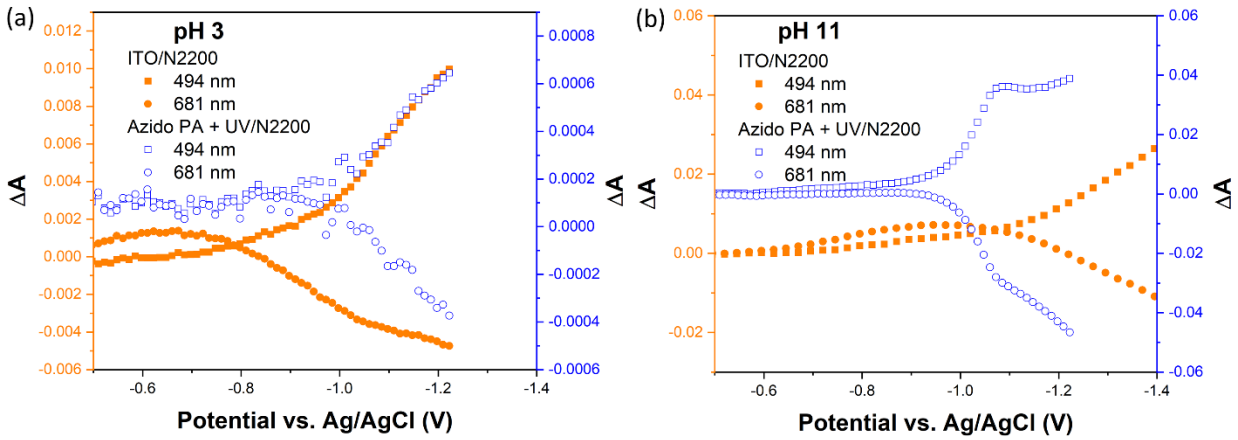

Fig. S16. The evolution of polaronic peak of N2200 at 494 nm and ground state bleach at 681 nm with respect to applied potential obtained from spectroelectrochemical experiment in (a) pH 3 and (b) pH 11.

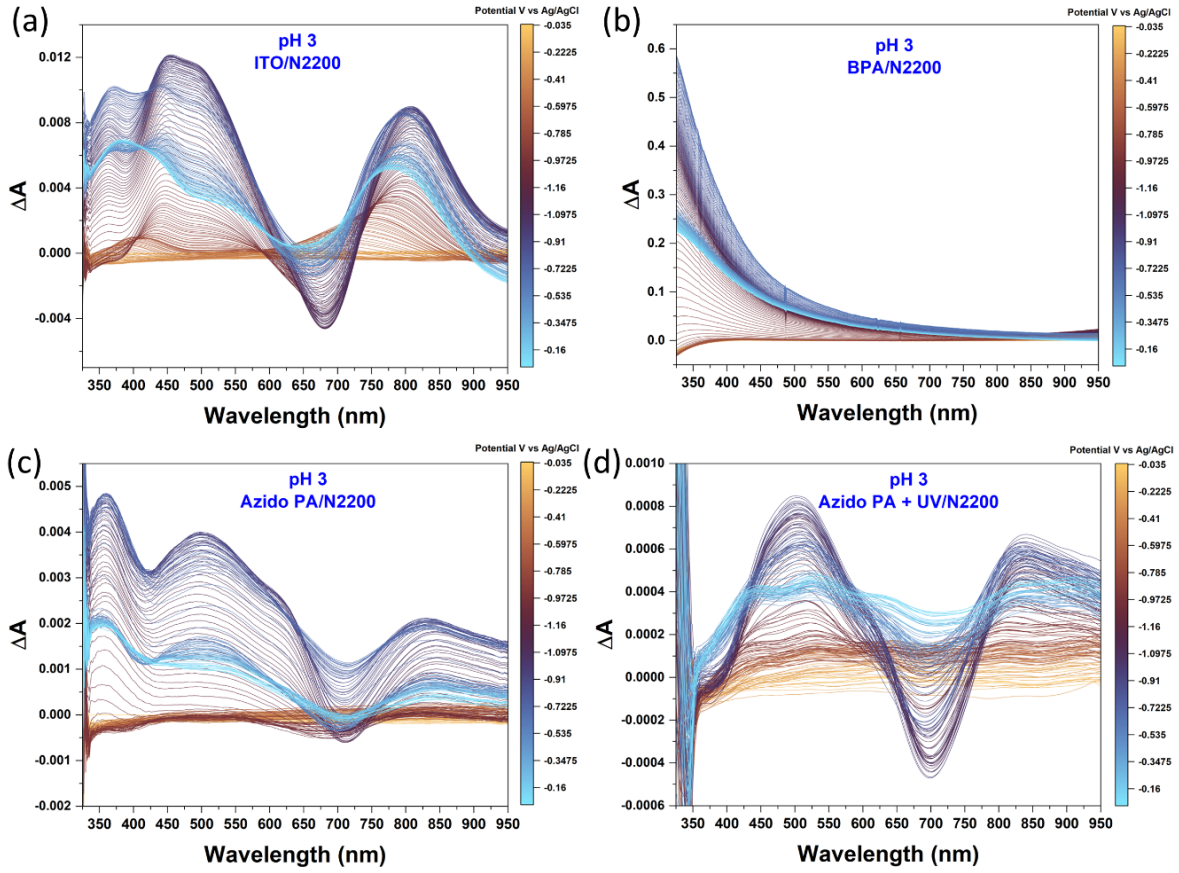

Fig. S17. Spectral evolution of the absorption of N2200 under negative sweeping potentials on (a) ITO; (b) ITO/BPA; (c) ITO/Azido PA and (d) ITO/Azido PA + UV at pH 3 with KCl as electrolyte. The ΔA is calculated by setting the initial film absorption as baseline. The data presented here are from the first CV cycle. ITO/N2200 film delaminated after first cycle, ITO/BPA/N2200 film delaminated during the first cycle.

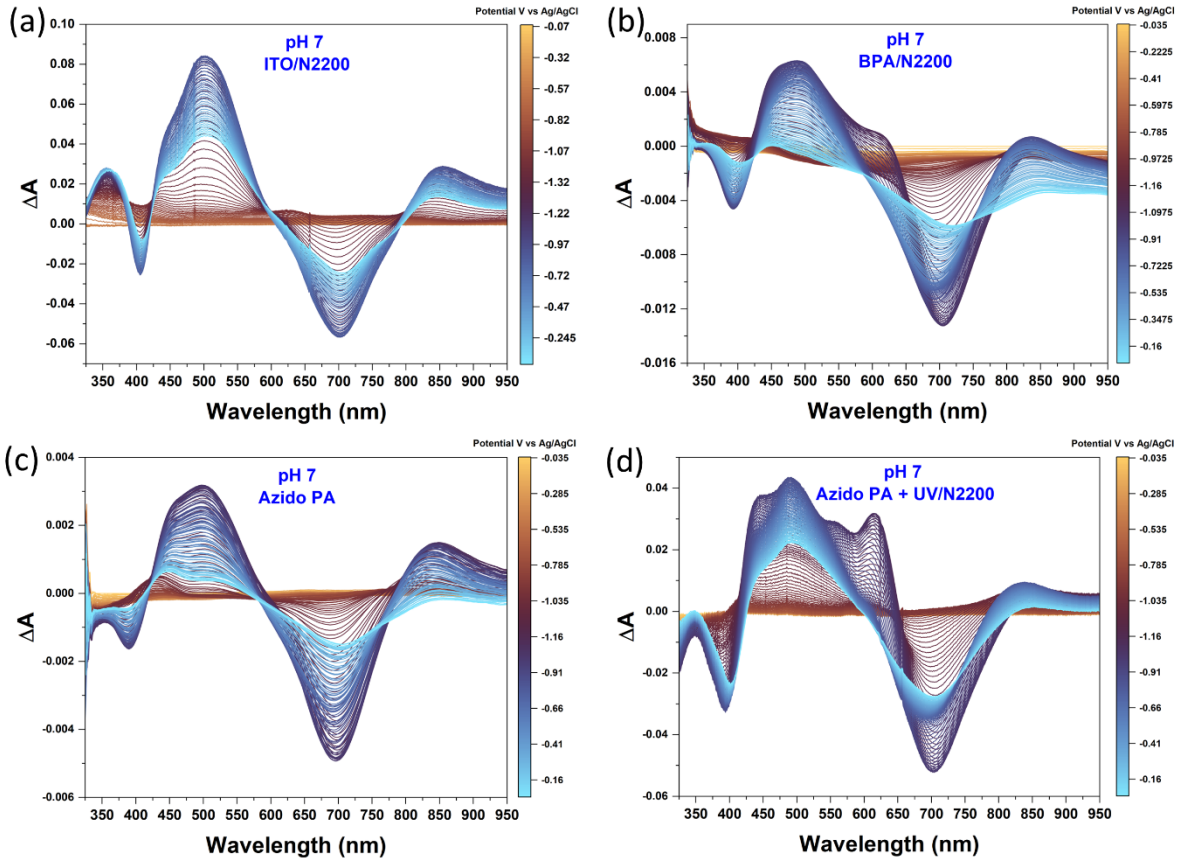

Fig. S18. Spectral evolution of the absorption of N2200 under negative sweeping potentials on (a) ITO; (b) ITO/BPA; (c) ITO/Azido PA and (d) ITO/Azido PA + UV at pH 7 with KCl as electrolyte. The ΔA is calculated by setting the initial film absorption as baseline. The data presented here are from the first CV cycle.

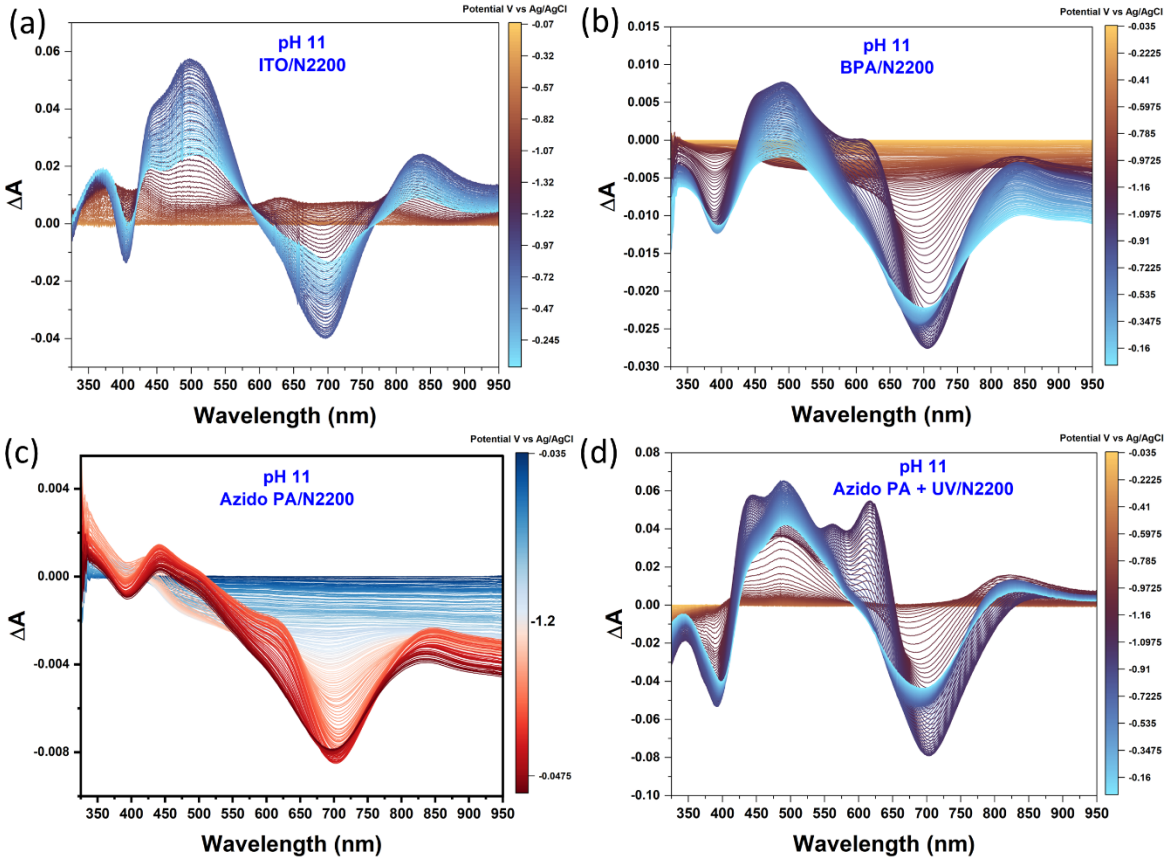

Fig. S19. Spectral evolution of the absorption of N2200 under negative sweeping potentials on (a) ITO; (b) ITO/BPA; (c) ITO/Azido PA and (d) ITO/Azido PA + UV at pH 11 with KCl as electrolyte. The ΔA is calculated by setting the initial film absorption as baseline. The data presented here are from the first CV cycle.

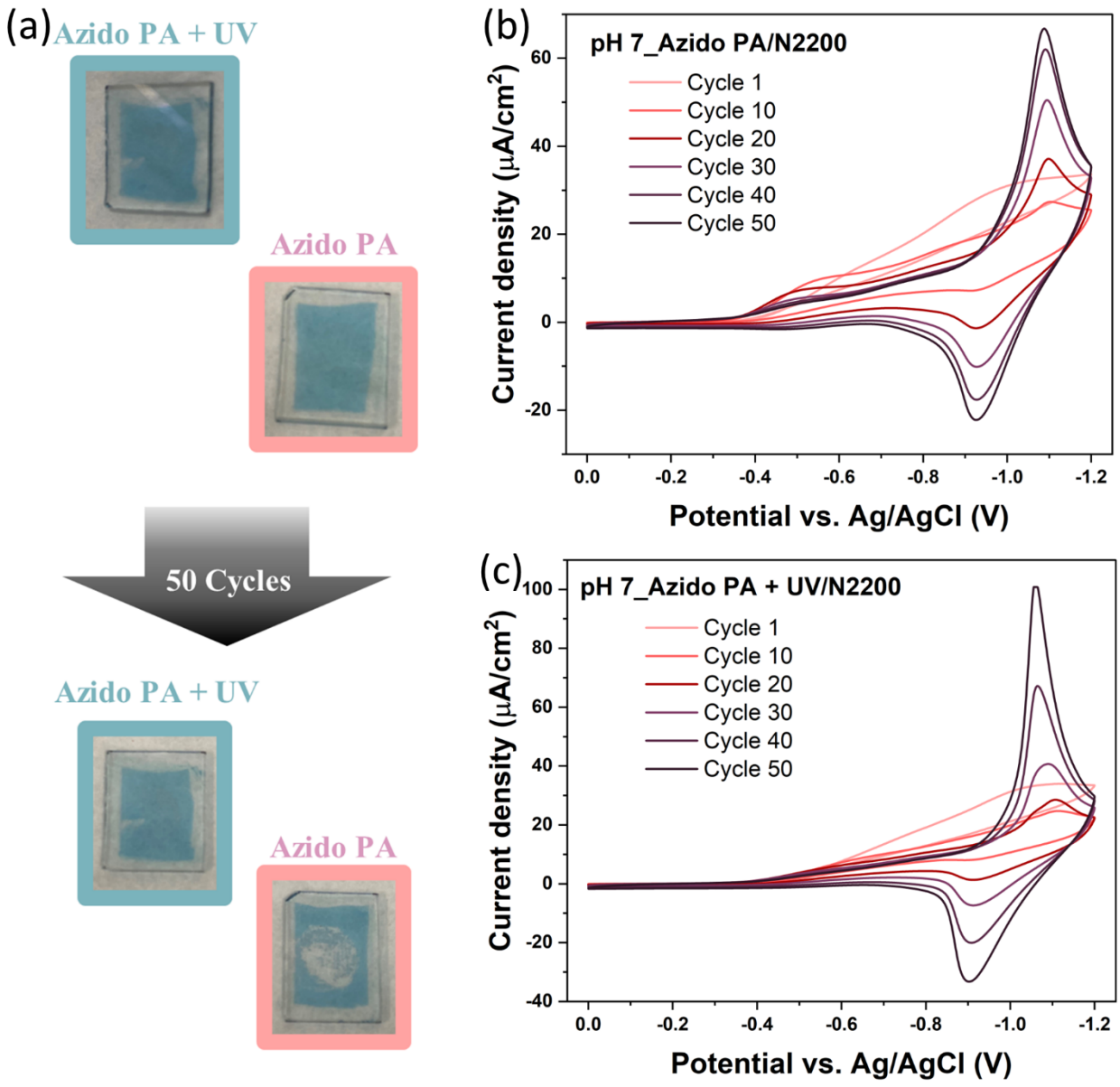

Fig. S20. (a) Photographs of the N2200 polymer films coated on Azido PA (with or without UV treatment) before and after 50 cycles of cyclic voltammetry in pH 7, the UV treated film looks more robust and shows no sign of delamination whereas the one without shows partial delamination. Cyclic voltammograms (up to 50 cycles) of N2200 on (b) Azido PA and (c) Azido PA with UV in aqueous medium.

None-Aqueous (Spectro)Electrochemical Data:

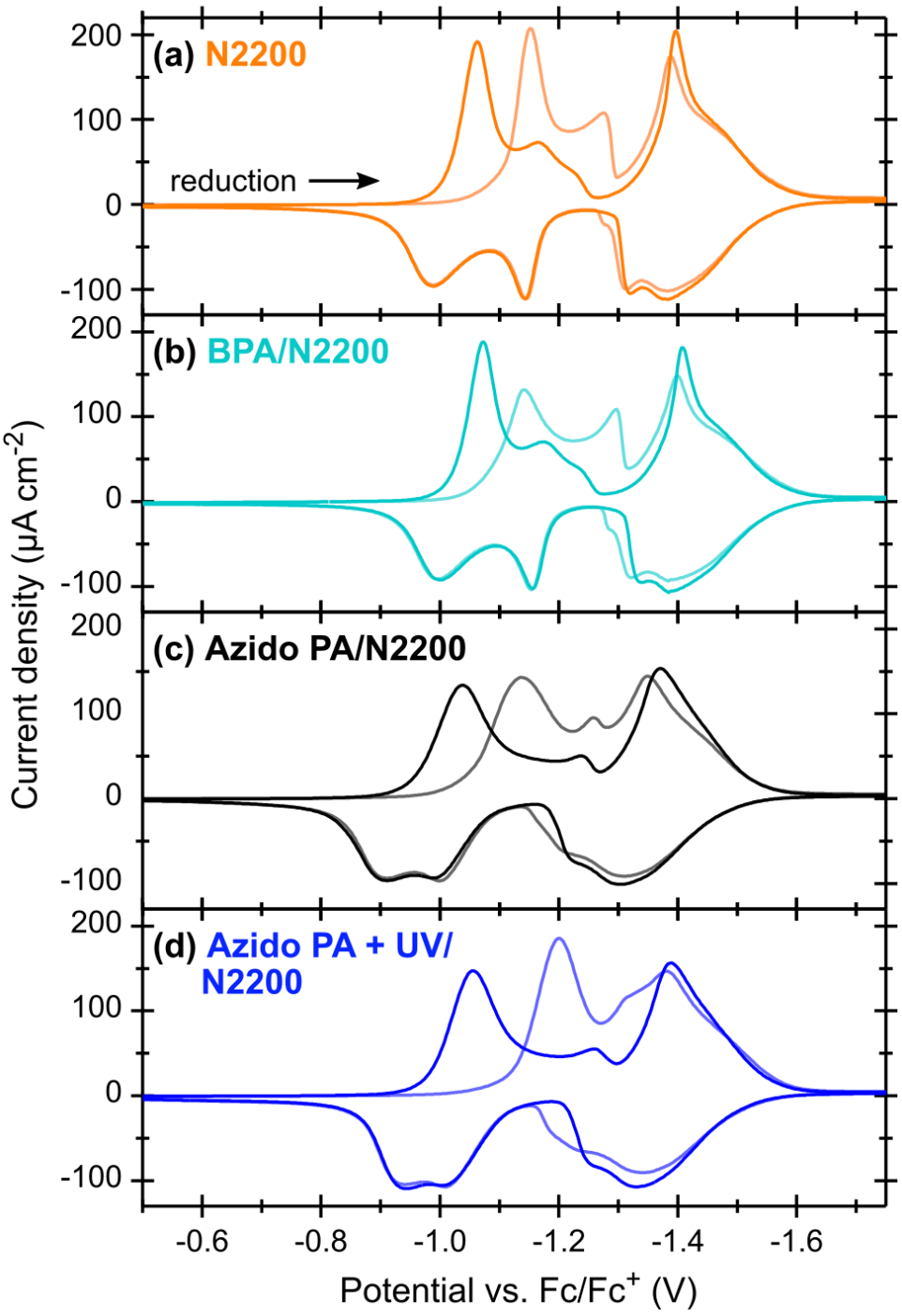

Fig. S21. First (light) and second (dark) cycles of non-aqueous CVs of N2200 films on ITO with various cross-linkers: (a) N2200 only, (b)BPA, (c) Azido PA, (d) Azido PA with UV treatment. All films show a distinct change from the first to second cycles, consistent with the incorporation of solvent and supporting electrolyte. US-convention CVs performed with N2200 films as working electrodes (masked to 1 cm^2), Ag/Ag^+ reference electrode, and Pt counter electrode, in acetonitrile with 100 mM $TBAPF_6$ supporting electrolyte at 20 mV/s. Potentials adjusted using a ferrocene/ferrocenium (Fc/Fc^+) standard.

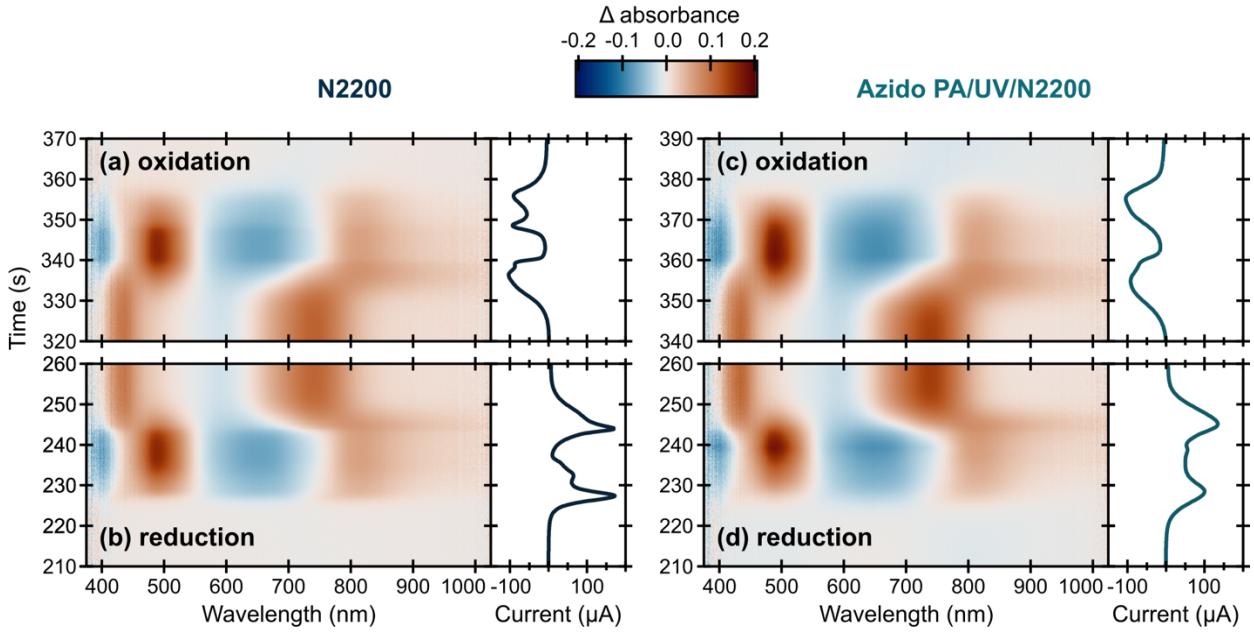

Fig. S22. Comparison of non-aqueous spectroelectrochemistry and accompanying current for (a,b) a N2200 film on ITO without any adhesion layer and (c,d) a N2200 film with UV-treated azido PA at the ITO interface. The Δ absorbance of the two different films are set to the same intensity scale. Electrochemical conditions are identical to those in Fig. 3; the data presented here are from the sixth CV cycle for each film.

References:

1 Y. Catel, M. Degrange, L. Le Pluart, P. J. Madec, T. N. Pham and L. Picton, *J. Polym. Sci. Part A Polym. Chem.*, 2008, **46**, 7074–7090.

2 P. J. Hotchkiss, S. C. Jones, S. A. Paniagua, A. Sharma, B. Kippelen, N. R. Armstrong and S. R. Marder, *Acc. Chem. Res.*, 2012, **45**, 337–346.

3 V. Christou, M. Etchells, O. Renault, P. J. Dobson, O. V. Salata, G. Beamson and R. G. Egdell, *J. Appl. Phys.*, 2000, **88**, 5180–5187.

4 S. Wu, *J. Adhesion*, 1973, **5**, 39–55.

5 S. Wu, *J. Polym. Sci. Part C Polym. Symp.*, 1971, **34**, 19–30.

6 D. K. Owens and R. C. Wendt, *J. Appl. Polym. Sci.*, 1969, **13**, 1741–1747.

7 F. M. Fowkes, *Ind. Eng. Chem.*, 2002, **56**, 40–52.